Proceedings of the 10th World Congress on Mechanical, Chemical, and Material Engineering (MCM'24)
Barcelona, Spain - August 22-24, 2024
Paper No. MMME 119
DOI: 10.11159/mmme24.119

Synergistic Effect of Corrosion and Wear for 6061 Aluminum alloy Electroless-plated with Ni-P and Ni-P-SiC layers

Che-Wei Lin, Yen-Ting Chen, Yin-Hsuan Chen, and Tung-Han Chuang
Department of Materials Science and Engineering, National Taiwan University, Taipei, Taiwan
chewei0820@gmail.com; a5331812@gmail.com ; tunghan@ntu.edu.tw
*Corresponding Author: tunghan@ntu.edu.tw

Abstract – 6061 aluminium alloy blocks were electroless-plated with Ni-P alloy layer and Ni-P-SiC layer. The distribution of ceramic SiC particles and the thickness of Ni-P-SiC were quite uniform which ensure the wear protection of this composite layer. Electrochemical tests in 3.5% NaCl aqueous solution show a sequence of corrosion potential: Ni-P-SiC > Ni-P > 6061 Al-alloy > anodic alumina film. On the other hand, the corrosion current density of these specimens shows a sequence of: anodic alumina film < Ni-P < Ni-P-SiC < 6061 Al-alloy. The hardness measurements reveal a sequence of: Ni-P-SiC > anodic alumina film > Ni-P > 6061 Al-alloy. The results of hardness are consistent with those of weight loss sequence after dry tests: Ni-P-SiC ~ anodic alumina film < < Ni-P < 6061 Al-alloy and corrosion-wear tests for 60 min: Ni-P-SiC ~ anodic alumina film < < Ni-P < < 6061 Al-alloy. In fact, the weight loss of electroless-plated Ni-P-SiC layer and anodic alumina film on 6061 Al-alloy are lower than 1 mg after both dry wear and corrosion-wear tests for 60 min, indicating a sound protection effect. Furthermore, the weight losses of 6061 Al alloy after corrosion-wear tests in 3.5% NaCl aqueous solution increased about 3 to 5 folds in comparison to those of dry wear tested results. An obvious synergistic effect has been observed in this case. However, the weight losses of anodic alumina film increased only 1.5 to 2 folds for the wear tests added with corrosion effect. More exciting is that only slight difference of weight losses occurred after dry wear tests and corrosion-wear tests for both electroless- plated Ni-P-SiC layer and anodic alumina film on 6061 Al-alloy, implying an ignorable influence of corrosion on wear damage.

Keywords: 6061 Aluminium alloy, Ni-P and Ni-P-SiC plating, corrosion, dry wear, corrosion- wear

1. Introduction

Among the various aluminum alloys, 6061 Al alloy with the main compositions of Al-Mg-Si possesses the advantageous of light weight, high strength good corrosion resistance and low cost, has been popularly applied in the constructional, architectural, and aeronautical workpieces [1, 2]. For the improvements of its corrosion and wear durability, anodic treatment was commonly used. In addition, Ni-P plating has been known as an effective protective layer for either wear or corrosion behaviors of aluminum alloys. Ni–P plating has garnered significant interest owing to their favorable mechanical and chemical properties, encompassing high hardness, strength, corrosion resistance, and wear resistance, among other attributes [3, 4]. Notably, Ni–P deposits exhibit an amorphous structure when the mass fraction of phosphorus is approximately 8% [5]. The deposit hardness demonstrates an upward trend with phosphorus content below this threshold, but it experiences a decline with further increases in phosphorus content [6]. Recently, SiC particles were added in the Ni-P layer to further increase its wear resistance[7, 9]. SiC particles could be incorporated into Ni–P matrix through direct current plating. As increasing the current density or the SiC concentration in the bath, the SiC content in the deposit correspondingly increases. In addition, adding SiC could substantially reduce the residual stress in the deposit and thus eliminate surface cracking. the addition of SiC leads to a substantial decrease in the phosphorus content in the deposit and then increases the hardness to a maximum of 770 Hv when the mass fraction of phosphorus in the deposit is about 3.7%. At higher phosphorus content, the deposits exhibit a preferential orientation of (1 1 1) Ni grains [9]. The wear resistance of an electroless co-deposited Ni-8.73% P-SiC coating was reported to be better than Ni-8.9% P, Ni-4.5% P-SiC, and electroplated chromium coatings. The superior wear resistance of the Ni-8.73% P-SiC coating is attributed to the SiC particles reducing the matrix grain size, enhancing the coating hardness, and resisting microcuts. The Ni-P alloy matrix, with a high phosphorus content, contributes to hardness and adequately supports the SiC. In comparison, the Ni-8.73% P-SiC coating exhibits greater wear resistance than the electroplated chromium coating, as the latter surface displays significant cracking, and its high hardness

diminishes rapidly at elevated temperatures [10].

Besides the damage of surface on aluminum caused by wear and corrosion, the synergistic effect resulted from the combination of corrosion and wear has drawn the attention of industry for many industrial alloys. It is known that wear can accelerate the corrosion failure due to the removal of anodic player, increasing the temperature and the activation of the aluminum surfaces. On the other hand, the hard corrosion products can also promote the wear rate. Aluminum alloy is prone to localized corrosion, such as pitting, intergranular, and exfoliation corrosion[11]. 6061 aluminum alloy is a precipitation-hardened alloy that incorporates magnesium and silicon as its primary alloying elements. In its T6 temper, 6061 exhibits an ultimate tensile strength of at least 290 MPa and a yield strength of at least 240 MPa. Corrosion is an ongoing concern and addressing or eliminating it proves to be a challenging task. Aluminium 6061 T6 alloy exhibits a higher corrosion rate in alkaline solutions compared to acidic solutions. Moreover, the corrosion resistance of the aluminum alloy is greater in solutions containing acids and salts with sulfate and nitrate ions than those with chloride ions [12]. Furthermore, the wear behavior of 6061 aluminum alloy holds significance in terms of economic and environmental factors[13]. The wear loss in 6061 aluminum alloy increased with higher applied loads, attributable to an augmented real contact area between the sliding surfaces under varying loads and elevated temperatures. The wear loss also showed an upward trend at all load levels examined as the temperature increased [14]. Combining the influence of both wear and corrosion phenomena, tribocorrosion is a degradation process affecting materials and is characterized by wear and corrosion [15, 16]. This phenomenon occurs in various settings, both in natural environments and industrial applications, where there is simultaneous exposure to mechanical contact and a corrosive environment [17]. The intricacy of tribocorrosion arises from the interdependence of chemical and mechanical degradation mechanisms. The coexistence of these mechanisms often results in accelerated material failure, driven by synergistic effects. Consequently, the overall material loss can be related to the material loss attributed to corrosion in the absence of wear or corrosion and the material loss resulting from the synergy between wear and corrosion[18, 19].The synergistic effect is particularly noticeable in passive alloys like aluminum, titanium, and stainless steels, which spontaneously form a protective thin oxide film (passive film) of a few nanometers in thickness when exposed to oxygen or water5,6. During the corrosion process, if this passive film is locally disrupted by mechanical wear, depassivation may occur, leading to localized corrosion and unexpected failures[20, 21].

This research focused on the corrosion and wear behaviors of Ni-P and Ni-P-SiC protective layers electroless-plated on 6061 aluminium alloy substrates. The microstructure of both electroless-plated Ni-P and Ni-P-SiC layers were observed and their hardness were measured. In addition, the corrosion behaviours of these specimens in aqueous 3.5% NaCl solution were analysed using electrochemical polarization method. Furthermore, the dry test and corrosion-wear test were conducted for the investigation of the synergistic effect of corrosion and wear for 6061 Al-alloy, anodic oxide film and electroless-plated Ni-P and Ni-P-SiC layers.

2. Experimental

6061 aluminium alloy cylindrical blocks were polished and electroless plated with Ni-P and Ni-P-SiC layers of 30 μm thickness. For comparison, anodic treated 6061 aluminium alloy specimens were also employed. The cross sections of the Ni-P and Ni-P-SiC layers on 6061 Al- alloy specimens were ground, polished and then observed via optical microscope (OM) and scanning electron microscopy (FEG-SEM, NOVA NANO SEM 450). In addition, the crystal structures of the Ni-P and Ni-P-SiC layers electroless-plated on 6061 Al alloy were identified by X-ray diffraction (XRD, Rigaku TTRAX). Furthermore, Transmission electron microscopy (TEM, FEI Tecnai G2 F20) was used for the microstructure analyses of the Ni-P and Ni-P-SiC layers electroless-plated on 6061 Al alloy. The microhardness of the 6061 Al-alloy, anodic oxide film, electroless-plated Ni-P and Ni-P-SiC layers was measured in accordance with ASTM E384. The measurement position was at the approximate center of the bonded specimen, the hardness was measured at 0.1 mm intervals at each point, and the measurement range extended from the center of the bonded interface to the left and right.

Wear and Wear-corrosion tests were conducted with a block-on-ring wear apparatus as shown in our previous papers [22, 23], for which dry wear tests in laboratory air and corrosion-wear tests in 3.5 wt.% NaCl solution open to air were performed. For the evaluation of corrosion behaviors of these anodic treated, Ni-P and Ni-P-SiC deposited 6061 aluminum alloy specimens in comparison with the bare 6061 alloy, electrochemical polarization measurements were conducted using a potentiostat with a platinum wire encircling the 6061 Al- alloy blocks as a counter electrode and a saturated calomel electrode as a reference electrode. The potentiostatic anodic polarization curves were obtained by applying potential from the open circuit potential to 0.5 V (SCE) at intervals of 0.1 V.

3. Results and Discussion

The cross-sectional micrograph of Ni-P-SiC composite layer electroless plated on 6061 Al- alloy was shown in Fig. 1. It can be seen in Fig. 1 that the silicon carbide particles with an average size about 0.3 μm were quite uniformly distributed in the electroless- plated Ni-P layer, which can ensure the wear and corrosion resistance of this composite layer. In addition, the thickness of the Ni-P-SiC composite layer was also quite uniform. These SiC ceramic particles are also uniformly distributed and partially exposed on the surface of the Ni-P-SiC composite layer electroless- plated on 6061 Al alloy as evidenced in Fig.2. It was also found in Fig. 1 that as the electrochemical reaction and deposition time during electroless-plating process increases, the local clustering phenomenon of these co-plated SiC ceramic particles appeared, and certain coarse silicon carbide particles with an average size about 1 μm might be embedded in the upper region of the Ni-P-SiC composite layer. It is believed that the coarser SiC particles have beneficial effect for the wear resistance of this electroless-plated Ni-P-SiC composite layer on 6061 aluminum alloy.

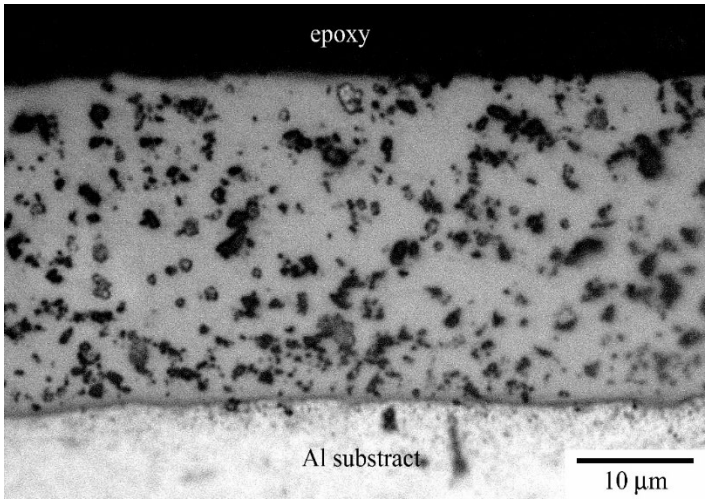

Fig.1 OM cross-sectional metallograph of SiC particles dispersed in Ni-P layer electroless-plated on 6061 Al-alloy.

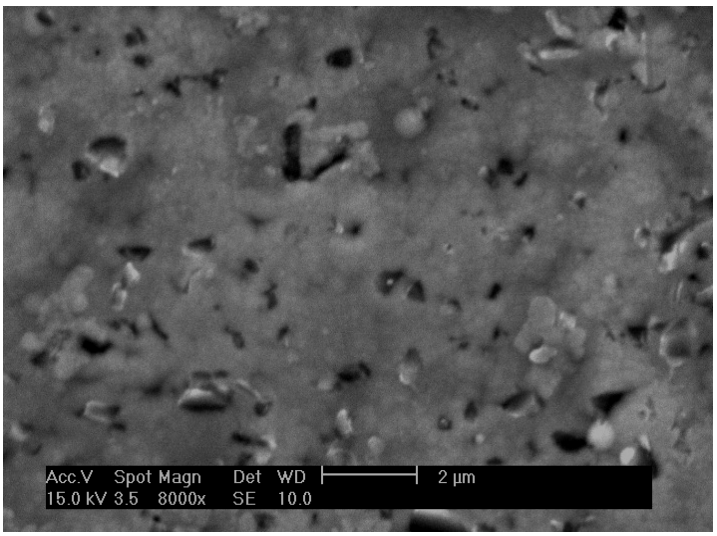

Fig.2 Top surface of electroless-plated Ni-P-SiC composite layer on 6061 Al-alloy.

The XRD analyses in Fig. 3 indicated that both Ni-P and Ni-P-SiC layers on 6061 aluminum alloy specimens under the electroless plating process have partially crystallinity. Figure 3a shows that the Ni-P layer possesses an FCC crystal structure. The phosphorus atoms are interstitially located in the nickel lattice to form an alloy solid solution. The co-plating of phosphorus with Ni can reduce the crystallinity of the Ni coating, and therefore the half-height width of the diffraction peak of Ni (111) peak becomes wider as evidenced in Fig. 3, implying the amorphous characteristic of Ni-P and Ni-P-SiC layers. The aluminium peaks can also be obviously observed in XRD analyses of Ni-P and Ni-P-SiC layers electroless-pated on 6061 Al alloy. Figure 3b shows certain α- SiC phase in XRD peaks. The appearance of these silicon carbide particles with HCP-crystal structure did not change the partially crystallinity of the nickel-phosphorus alloy.

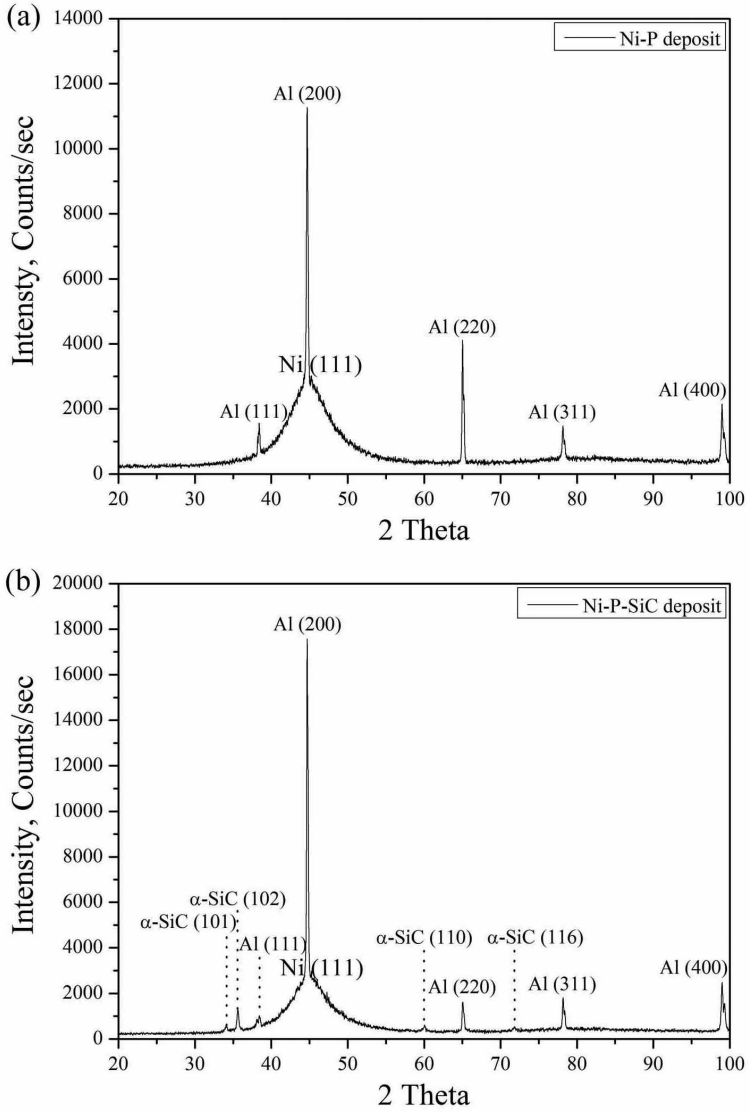

Fig. 3 XRD analyses of (a) Ni-P layer and (b) Ni-P-SiC composite layer electroless-plated on 6061 Al-alloy.

The microstructure, crystallinity and composition of electroless-plated Ni-P and Ni-P-SiC layers were further investigated with TEM. The observations were especially emphasized on the precipitation reaction of Ni-P alloy and the bonding effect of silicon carbide ceramic with Ni-P matrix. Figure 4 shows that the electroless Ni-P alloy layer has a fine equiaxed crystal structure. It can be observed in bright and dark fields that there are plane defects with parallel stripes inside the Ni-P electroless plating grains (Fig.4a). Such crystal defects have a twin structure and will especially appeared in larger precipitates. The crystallinity of the electroless nickel-phosphorus coating was analysed by selective area electron diffraction

(SAED). Figure 4c shows a ring-shaped diffraction pattern. For comparison, the plane spacing of each diffraction ring is consistent with the crystal structure of FCC nickel. The composition analysis in Fig. 4d indicates that the phosphorus content of the electroless plated Ni-P alloy layer is about 7 wt.%.

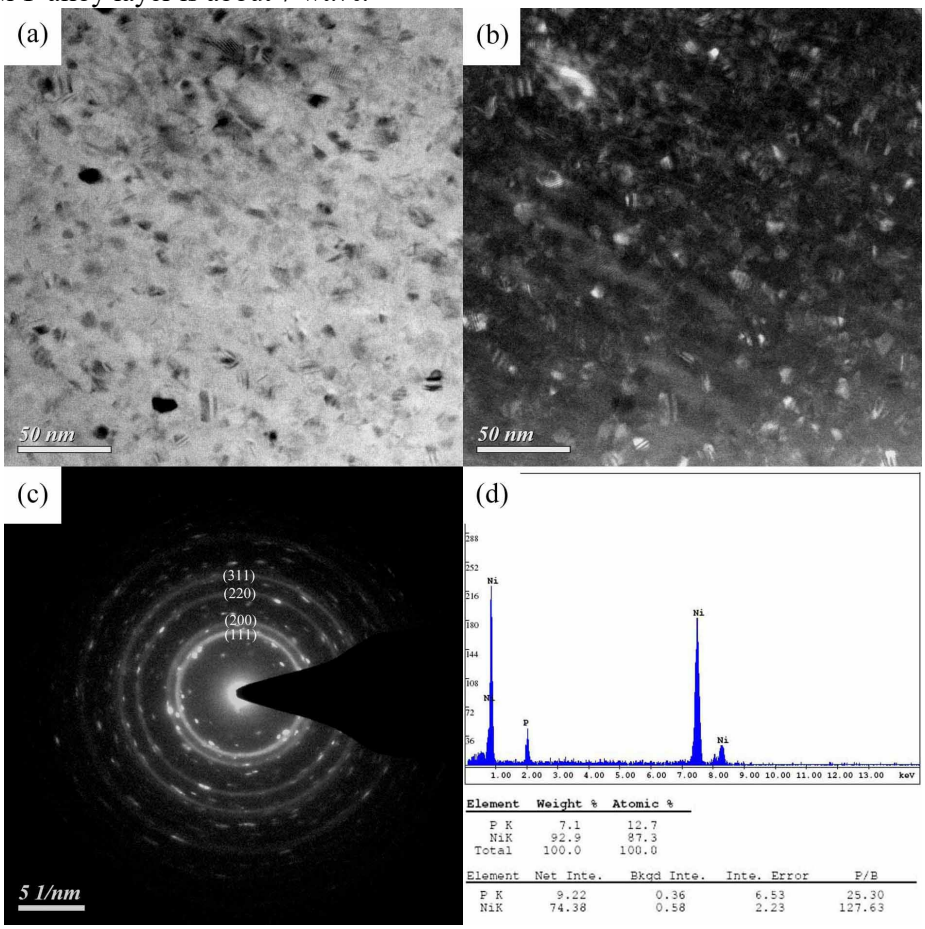

Fig. 4 TEM micrographs of the Ni-P layer electroless-plated on 6061 Al-alloy：(a) bright field image, (b) dark field image, (c) electron diffraction pattern, (d) EDX- alloy composition analysis.

Figures 5 and 6 show the TEM microstructures of the electroless- plated Ni-P-SiC composite layer on 6061 Al- alloy. The bright and dark fields of Figure 5 show that the micron-sized silicon carbide and the nanocrystalline nickel phosphorus base are well bonded, and no crevice can be found at the interface between SiC particle and Ni-P matrix. However, Gap defects can be observed as the SiC particles clustered as shown in Fig. 5c. Figure 6 shows that the Ni-P-SiC composite layer tightly bonded with 6061 Al-alloy, leading to an excellent interface. selective area electron diffraction (SAED) indicates the partially crystallinity of Ni-P phase. In Fig. 6b, it was found that a SiC-depleted region appeared in the Ni-P-SiC composite layer near the 6061 Al-alloy substrates. This phenomenon implied that the SiC ceramic particles are not easily co-plated with the Ni-P alloy at the early stage of the electroless plating process for Ni-P-SiC composite layer on 6061 aluminium alloy.

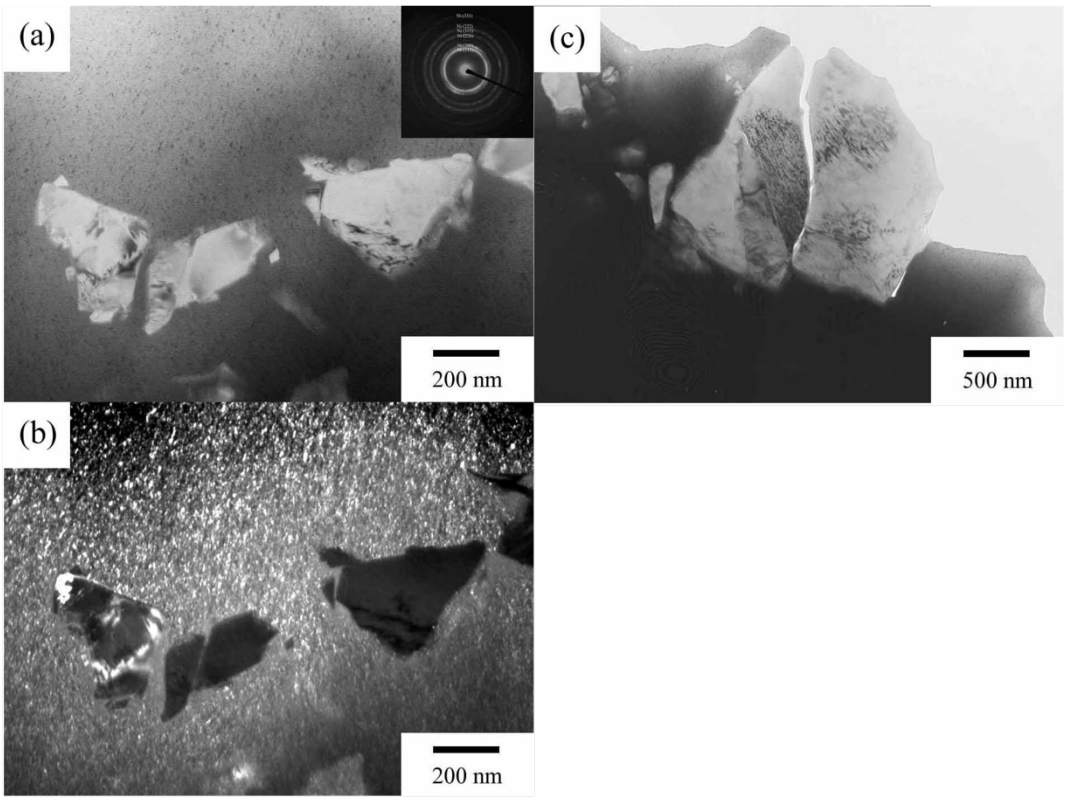

Fig. 5 TEM micrographs of the Ni-P-SiC composite layer electroless-plated on 6061 Al-alloy electroless plated nickel-phosphorus-silicon carbide composite layer： (a) bright field image, (b) dark field image, (c) nickel phosphorus matrix/silicon carbide interface.

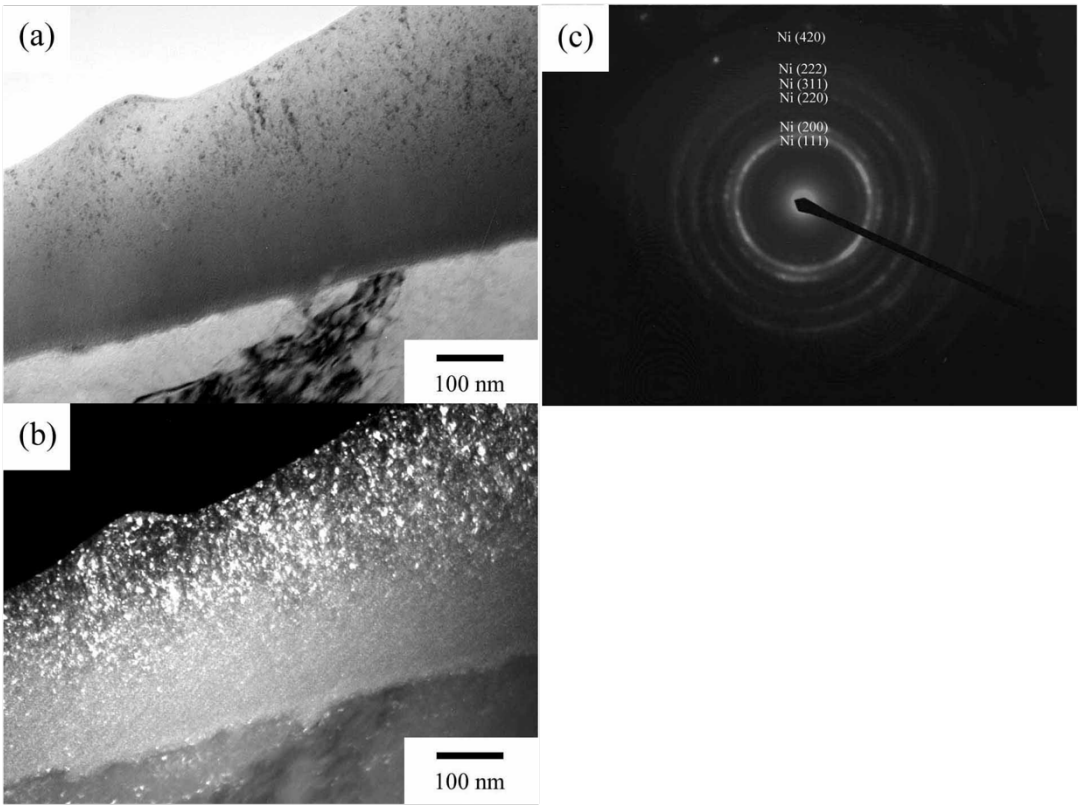

Fig. 6 TEM micrographs at the interface between Ni-P-SiC layer and 6061 Al-alloy substrate: (a) bright field image, (b) dark field image, (c) electron diffraction pattern.

Figure 7 shows the potentiodynamic polarization curves of 6061 aluminium alloy, anodic alumina film, electroless-plated Ni-P and Ni-P-SiC layers in aqueous 3.5 wt.% NaCl solution. The corrosion potential (Φ_{corr}) of these specimens taken from the polarization curves were listed in Table I, which shows a sequence of: Ni-P-SiC **>** Ni-P **>** 6061 Al-alloy **>** anodic alumina film. It was also found that the Ni-P-SiC composite layer has a more noble corrosion potential near that of Ni-P layer on 6061 Al-alloy, while the corrosion potential of more active 6061 Al-alloy is near that of anodic oxide film on 6061 Al-alloy. The corrosion current density (I_{corr}) can also be obtained from the polarization plots in Fig. 7, which are also summarized in Table I. It can be seen in Fig. 7 and Table I that the corrosion current density of these specimens shows a sequence of: anodic alumina film < Ni-P < Ni-P-SiC < 6061 Al-alloy, which indicates that the 6061 Al-alloy has the highest corrosion rate. In addition, the electroless- plated Ni-P and Ni-P-SiC layers show higher corrosion tendency than that of anodic oxide film of 6061 Al-alloy. The results in Fig. 7 also indicate that the addition of SiC particles in Ni-P layer did not affect the corrosion potential and corrosion rate of the electroless plated layers on 6061 Al-alloy.

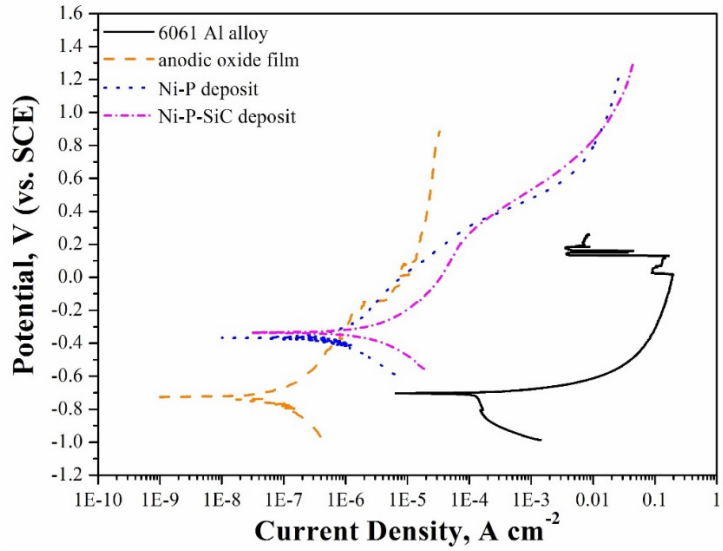

Fig. 7 Potentiostatic polarization curves of 6061 Al-alloy, anodic oxide film, electroless-plated Ni-P and Ni-P-SiC layers in 3.5% NaCl solution.

Table I. Corrosion potential (Φ_{corr}) and corrosion current density (I_{corr}) in 3.5 % NaCl solution, and Vickers hardness, and weight losses after wear tests for 60 min (dry wear and corrosion-wear) for 6061 Al-alloy, anodic oxide film, electroless-plated Ni-P and Ni-P-SiC layers.

	6061 Al-alloy	**Anodic Oxide Film**	**Ni-P Layer**	**Ni-P-SiC Layer**
Corrosion Potential (mV)	-695	-706	-358	-330
Corrosion Current Density (uA/cm^2)	180	0.5	1.1	2.3
Vickers Hardness (Kg/mm^2)	100	420	385	550
Weight Loss Dry Wear (g)	26	2.5	22	2.1
Weight Loss Corrosion-Wear (g)	140	2.8	42	2.4

Figure 8 shows the Vickers hardness of the 6061-aluminium alloy, anodic alumina film, electroless-plated Ni-P and Ni-P-SiC layers in this study. The results are also summarized in Table I, which reveals a sequence of: Ni-P-SiC **>** anodic

alumina film > Ni-P > 6061 Al-alloy. In fact, the hardness of Ni-P electroless-plated layer is quite near to that of anodic alumina film, and both are relatively lower than that of Ni-P-SiC composite layer. In contrast, the 6061 aluminium has a quite low hardness in comparison to those of the anodic alumina film, electroless-plated Ni-P and Ni-P-SiC layers in this study. From the hardness measurements, it can be expected that the anodizing treatment and electroless-plating Ni-P and Ni-P-SiC layers can effectively improve the wear resistance of the 6061 aluminum alloy. It is evidenced in Fig.9 to show the plots of weight losses for 6061 Al-alloy, anodic alumina film, electroless-plated Ni-P and Ni-P-SiC layers after dry wear tests and corrosion-wear tests in 3.5 % NaCl solution. The data of both wear and corrosion-wear tests for 60 min are summarized in Table I for the comparison. From the dry wear tests, a sequence of weight losses is obtained: Ni-P-SiC ~ anodic alumina film < < Ni-P < 6061 Al-alloy. It is interesting that the tendency of weigh losses after dry wear tests is quite consistent with that of the measurements of Vickers hardness for these specimens. Similarly, the weight losses after corrosion-wear tests in aqueous 3.5 % NaCl solution for 6061-aluminium alloy, anodic alumina film, electroless-plated Ni-P and Ni-P-SiC layers reveal a sequence of: Ni-P-SiC ~ anodic alumina film < < Ni-P < < 6061 Al-alloy. More exciting is that the weight loss of electroless-plated Ni-P-SiC layer and anodic alumina film on 6061 Al-alloy are lower than 1 mg after both dry wear and corrosion-wear tests for 60 min, indicating a sound protection effect. From Fig. 9a and Fig. 9b, it can also be found that the weight losses of 6061 Al alloy after corrosion-wear tests in 3.5% NaCl aqueous solution increased about 3 to 5 folds in comparison to those of dry wear tested results for 20 to 60 min. The results confirmed the synergistic effect of corrosion and wear. However, the weight losses of anodic alumina film increased only 1.5 to 2 folds for the wear tests added with corrosion effect. For both electroless- plated Ni-P-SiC and anodic alumina film on 6061 Al-alloy, the weight losses after dry wear tests and corrosion-wear tests are almost unchanged, implying a minor influence of corrosion on wear damage.

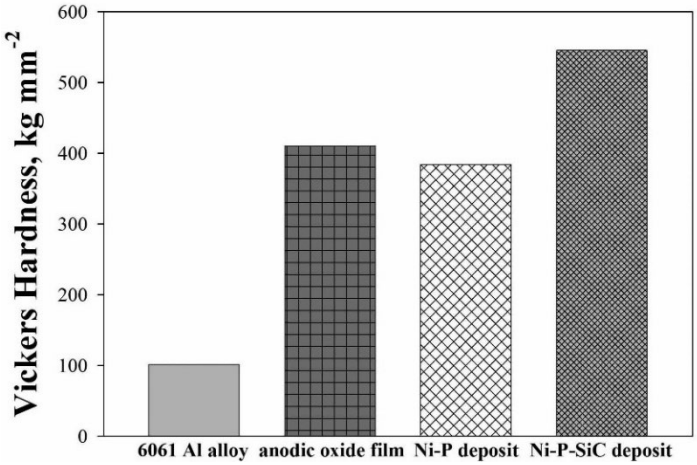

Fig. 8 Comparison of microhardness for 6061 Al-alloy, anodic oxide film, electroless-plated Ni-P and Ni-P-SiC layers.

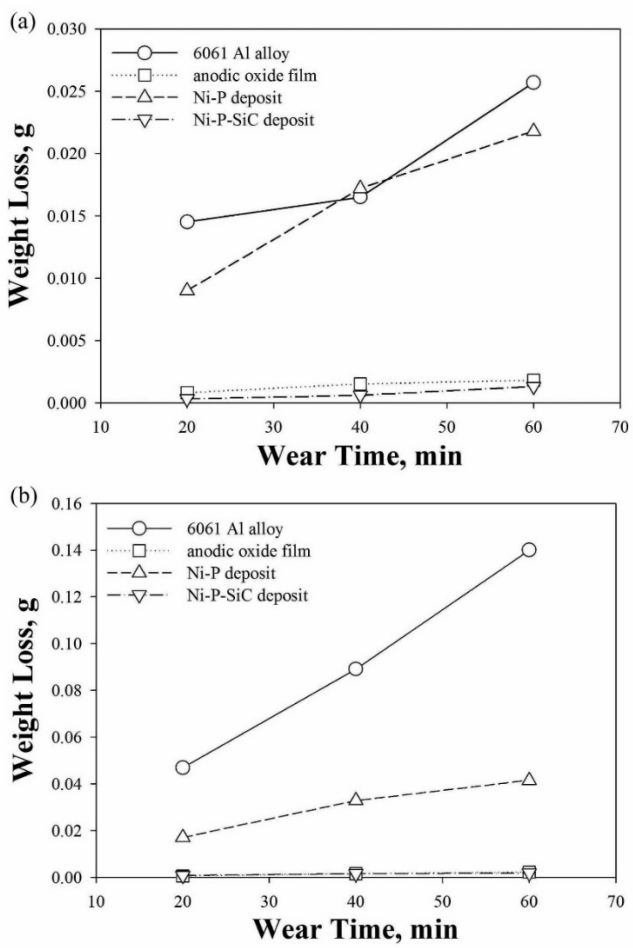

Fig. 9 Weight loss of 6061 Al-alloy, anodic oxide film, electroless-plated Ni-P and Ni-P-SiC layers after (a) dry wear test and (b) corrosion-wear test in 3.5% NaCl.

The cross-sectional morphology of 6061 Al-alloy, anodic oxide film, electroless-plated Ni-P and Ni-P-SiC layers after dry wear test and corrosion-wear test in 3.5% aqueous NaCl solution are shown in Fig. 10 and 11, respectively. It is found that the anodic film, Ni-P and Ni-P-SiC layers adhered well to the 6061 Al alloy substrates and the thinning of the plating layers are quite uniform. Figure 10d reveals many Ni-P fragments on the dry worn surface of Ni-P-SiC layer after dry wear tests, indicating that certain SiC particles broke away from the Ni-P-SiC composite layer. Most of these Ni-P fragments dissolved and dropped out with the SiC particles after corrosion-wear tests as shown in Fig. 11d. In addition, Fig. 11 shows that certain corrosion products appeared on the surfaces of 6061 Al-alloy, anodic film, Ni-P and Ni-P-SiC layers after corrosion-wear tests. In comparison to the cross-sections in Figures 10c after dry wear tests, the remained Ni-P electroless-plated layer in Figures 11c are much thinner after corrosion-wear tests. The more severe abrasion of corrosion-worn Ni-P layer in comparison to that after dry wear tests can further verify the synergistic of corrosion and wear for electroless-plated Ni-P layer.

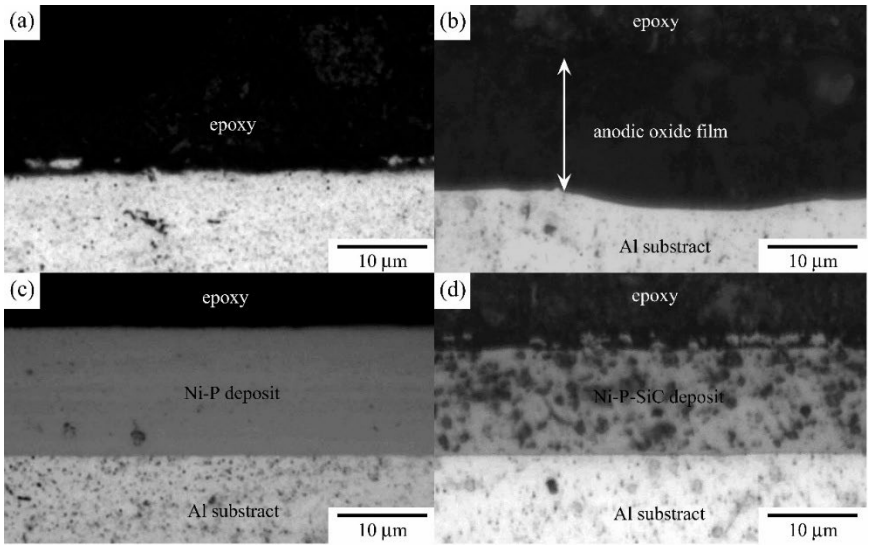

Fig. 10 Cross-sectional morphology of (a) 6061 Al-alloy, (b) anodic oxide film, (c) Ni-P and (d) Ni-P-SiC layers after dry wear tests.

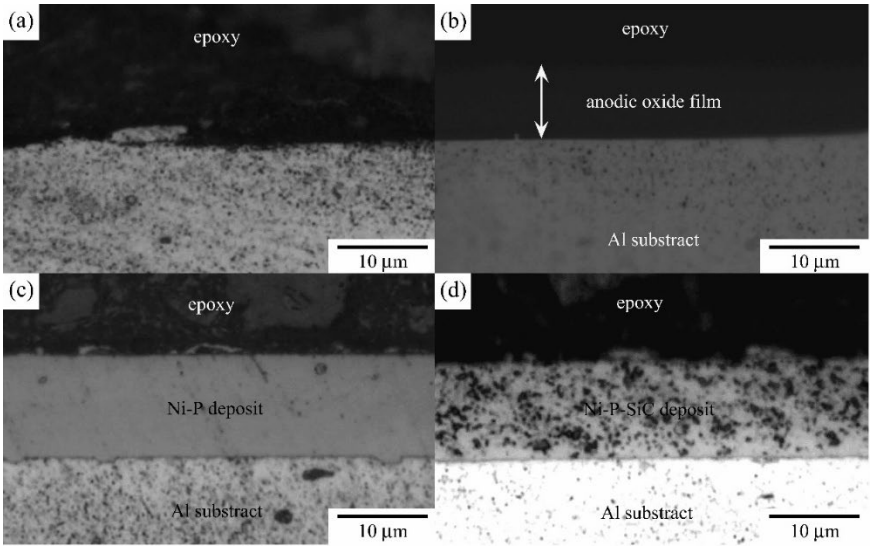

Fig. 11 Cross-sectional morphology of (a) 6061 Al-alloy, (b) anodic oxide film, (c) Ni-P and (d) Ni-P-SiC layers after corrosion-wear test in 3.5% NaCl.

4. Conclusions

Anodic treatment and electroless plated Ni-P and Ni-P-SiC layers for 6061 aluminium alloy can effectively reduce the corrosion potential and corrosion current density of 6061 Al-alloy, improving its corrosion tendency and corrosion rate in aqueous 3.5 % NaCl solution. The Ni-P-SiC composite layer shows a very high Vickers hardness of 550 kg/mm^2, leading to the lowest weight losses and good wear resistance after both dry wear and corrosion wear tests. The drastic acceleration of weight loss for 6061 Al alloy from 26 g after dry wear test for 60 min to 140 g after corrosion-wear test, indicated a severe synergistic effect of corrosion and wear. In contrast, such an accelerating phenomenon of wear rate did not occur for both Ni-P-SiC electroless-plated layer and anodic oxide film after corrosion-wear tests in 3.5 % NaCl solution. Summarizing the results in this study, electroless-plating Ni-P-SiC composite layer on 6061 aluminium alloy can effectively improve its corrosion, wear and corrosion-wear behaviours.

Acknowledgement

This study was sponsored by Yung-Chi Paint & Varnish MFG. Co. LTD and the industrial and academic cooperation programs of SHENMAO Technology Inc. and the Ministry of Science and Technology, Taiwan, under Grant No. NSTC-112-2622-E-002-037. It was also sponsored by the Emerging Technology Application Program of the Hsinchu Science Park R&D program of Ag Materials Technology Co., LTD, under Grant No. 112AO03A.

Author Contributions: Experimental, Che-Wei Lin; Results discussion and paper writing, Yen-Ting Chen and Yin-Hsuan Chen; Conceptualization, supervision, and project administration, Prof. Tung-Han Chuang.

References

[1] A. M. Kuhlmann, (1963). The second most abundant element in the earth's crust. JOM, 15(7), 502-505.

[2] Abd El-Hameed, A. M., & Abdel-Aziz, Y. A. (2021). Aluminium Alloys in Space Applications: A Short Report. J. Appl. Sci. Eng., 22(1), 1-7.

[3] C. Y. Liue, J. W. Wang, Y. M. Peng, H. J. Chen, and J. H. Shen, "Ni-SiC composite plating," *MRL Bulletin of Research and Development;(Taiwan)*, vol. 4, 1990.

[4] M. Ghouse, "Wear characteristics of sediment co-deposited nickel-SiC composite coatings," *Metal finishing*, vol. 82, no. 3, pp. 33–37, 1984.

[5] D. B. Lewis and G. W. Marshall, "Investigation into the structure of electrodeposited nickel-phosphorus alloy deposits," *Surf Coat Technol*, vol. 78, no. 1–3, pp. 150–156, 1996.

[6] R. Weil, J. H. Lee, I. Kim, and K. Parker, "Comparison of Some Mechanical and Corrosion Properties of Electroless and Electroplated Nickel--Phosphorus Alloys," *Plat. Surf. Finish.*, vol. 76, no. 2, pp. 62–66, 1989.

[7] X. Fu, F. Wang, X. Chen, J. Lin, and H. Cao, "Corrosion resistance of Ni–P/SiC and Ni–P composite coatings prepared by magnetic field-enhanced jet electrodeposition," *RSC Adv*, vol. 10, no. 56, pp. 34167–34176, 2020.

[8] Tsongas, K., Tzetzis, D., Karantzalis, A., Banias, G., Exarchos, D., Ahmadkhaniha, D., ... & Bochtis, D., "Microstructural, surface topology and nanomechanical characterization of electrodeposited Ni-P/SiC nanocomposite coatings," *Applied Sciences*, vol. 9, no. 14, p. 2901, 2019.

[9] M.-C. Chou, M.-D. Ger, S.-T. Ke, Y.-R. Huang, and S.-T. Wu, "The Ni–P–SiC composite produced by electro-codeposition," *Mater Chem Phys*, vol. 92, no. 1, pp. 146–151, 2005, doi: https://doi.org/10.1016/j.matchemphys.2005.01.021.

[10] H. Xinmin and D. Zongang, "The wear characteristics of Ni-P-SiC composite coatings," *Transactions of the IMF*, vol. 70, no. 2, pp. 84–86, 1992.

[11] F. Andreatta, H. Terryn, and J. H. W. de Wit, "Corrosion behaviour of different tempers of AA7075 aluminium alloy," *Electrochim Acta*, vol. 49, no. 17, pp. 2851–2862, 2004, doi: https://doi.org/10.1016/j.electacta.2004.01.046.

[12] S. Ranjith Kumar, S. Dinesh Krishnaa, M. Dinesh Krishna, N. T. Gokulkumar, and A. R. Akilesh, "Investigation on corrosion behaviour of aluminium 6061-T6 alloy in acidic, alkaline and salt medium," *Mater Today Proc*, vol. 45, pp. 1878–1881, 2021, doi: https://doi.org/10.1016/j.matpr.2020.09.079.

[13] H. Ye, "An overview of the development of Al-Si-alloy based material for engine applications," *J Mater Eng Perform*, vol. 12, pp. 288–297, 2003.

[14] S. Athula, G. Premnatha, B. Sunilb, and V. R. Rajeev, "Elevated temperature wear behaviour of aluminium alloy (Al 6061)," in *Proceedings of the National Conference on Latest Trends in Mechanical Engineering, NCLTME, Palakkad, Kerala, India*, 2011.

[15] ASTM Standard., "Standard Guide for Determining Synergism Between Wear and Corrosion," 2016

[16] D. Landolt and S. Mischler, *Tribocorrosion of passive metals and coatings*. Elsevier, 2011.

[17] H.H. Huang, and T.H. Chuang, "Erosion- and wear-corrosion behaviour of Fe-Mn-Al alloys in NaCl solution," Mater. Sci. Eng. A, 292 (2000) 90-95.

[18] S. Mischler, "Sliding tribo-corrosion of passive metals: mechanisms and modeling," in *Third International Symposium on Tribo-Corrosion*, ASTM international, 2013, pp. 1–18.

[19] D. Landolt, S. Mischler, and M. Stemp, "Electrochemical methods in tribocorrosion: a critical appraisal," *Electrochim Acta*, vol. 46, no. 24–25, pp. 3913–3929, 2001.

[20] D. Wolf, V. Yamakov, S. R. Phillpot, A. Mukherjee, and H. Gleiter, "Deformation of nanocrystalline materials by molecular-dynamics simulation: relationship to experiments?" *Acta Mater*, vol. 53, no. 1, pp. 1–40, 2005.
[21] J. Chen, H. Mraied, and W. Cai, "Determining tribocorrosion rate and wear-corrosion synergy of bulk and thin film aluminum alloys," *JoVE (Journal of Visualized Experiments)*, no. 139, p. e58235, 2018.
[22] C.K. Fang, C.C. Huang, and T.H.Chuang, "Synergistic effects of wear and corrosion for Al2O3 particulate-reinforced 6061 aluminium matrix composites," Metall. And Mater. Trans., A, 30 (1999) 643-651.
[23] S.Y. Yu, H. Ishii, and T.H. Chuang, "Corrosion wear of SiC whisker- and particulate- reinforced 6061 aluminum alloy composites," Metall. And Mater. Trans., A, 27 (1996) 2653-2662.